

# Approaches to Cleaning Gas Response Signals from Metal Oxide Sensors

## Optimisation and Generalizability

Jacqueline Whalley, Philip Sallis

Engineering, Computer and Mathematical Sciences  
Auckland University of Technology  
Auckland, New Zealand  
e-mail: {jwhalley, psallis}@aut.ac.nz

Enobong Bassey

Geography, Environment and Disaster Management  
Coventry University  
Coventry, England  
e-mail: enobong.bassey@coventry.ac.uk

**Abstract**—This paper reports on a comparative analysis of techniques – from simple polynomial curve fitting to digital filters, local regression and wavelet denoising – for cleaning thin film composite metal oxide gas sensor response signals. This research expands and extends a preliminary investigation of simple methods for smoothing metal oxide gas sensor response signals. As part of the analysis an extensive series of systematic experiments were conducted in order to tune the parameters, including span or frame sizes and degrees of polynomial as appropriate, for each of the digital filters and to select the appropriate mother wavelet and threshold chooser for the wavelet approach. The signal processing challenge of maintaining a balance between the measured signal variation and the disparity variation in the smoothed signal is outlined and considered in comparing the performance of the signal cleaning methods. The results indicate that a Savitsky Golay filter with a polynomial degree of 3 and a frame size of 9% of a signal's width provides a practical solution for denoising metal oxide gas sensor signals because it was found to consistently give a cleaned signal that is suitable for further processing (feature extraction and pattern recognition). This work provides support for the premise that a generalized method for cleaning metal oxide gas sensor signals, regardless of sensor composition, is possible and suggests that a Savitsky Golay filter is a suitable candidate.

**Keywords**—*Denoising; Wavelets; Savitsky Golay filter; Frame Size; Polynomial; Metal Oxide Sensors.*

### I. INTRODUCTION

This research expands and extends a preliminary investigation of simple methods for smoothing metal oxide gas sensor response signals [1]. Precise and reliable measurements of trace gases such as carbon monoxide (CO), nitrous oxide (NO), sulfur dioxide (SO<sub>2</sub>) carbon dioxide (CO<sub>2</sub>), methane (CH<sub>4</sub>) and other hydrocarbons [2] are essential for environmental monitoring. Such gases are harmful not only to the environment but also to human health if present beyond certain concentrations [3]. Local, national and international legislation requires continuous monitoring of air quality and rate of emissions. This emissions data is critical to the decision making and formulation of policies related to climate change. As a consequence, there has been considerable effort focused on the fabrication of low cost, portable, reliable and accurate sensors for monitoring such

gases. For the measurements obtained from these sensors to be accurate, reliable and interpretable some processing of the raw signal is required. A useful summary of statistical and optimization methods that have been used to process gas sensor array signals is provided by Gutierrez-Galvez [4].

The signal processing of gas sensor data has four key steps: *pre-processing*, *dimensionality reduction*, *prediction*, and *validation* [5]. This work focuses on the pre-processing phase; which facilitates noise elimination, data smoothing/filtering and signal enhancement; with the sole aim of increasing the signal-to-noise ratio without greatly distorting the original response signal.

In sensor systems noise has several possible sources introduced at various points in the measurement process. Several forms of noise are irreducible because they are inherent to the underlying electronic components or physical properties of the sensor [6]. Other forms of noise originate from processes and include 1/f noise, quantization and transmission noise [7]. The most harmful noise is the noise that is propagated in the early stages of measurement and, therefore, can be propagated and amplified through the later stages in the signal pathway [8].

One approach to producing a clean signal would be to use physical filters. While physical filters have been shown to produce cleaner signals they do not cover the full resolution and shape of the curve [1]. This is problematic because in order to improve the interpretability, sensitivity and selectivity of the measurements from metal oxide (MOX) gas sensor array signals it is preferable to use the full resolution and profile of the signal. An alternate approach to physical filters is to use a digital filter to clean the signal. If taking this approach the choice of signal pre-processing method is critical because it has a significant impact on the overall final quality of the processed signal [7].

This paper reports on a systematic series of experiments that were conducted in order to compare various computational methods for the smoothing or denoising of MOX gas sensor response signals using digital filtering approaches. For each method a comprehensive and systematic set of experiments was conducted in order to tune the parameters for the method. The aim was to establish a general method and guidelines for the signal pre-processing phase (denoising phase) of responses from SnO<sub>2</sub>-ZnO devices regardless of composition. The rest of this paper is organized as follows. Section II discusses the relevant

background research into the denoising and smoothing of chemical sensor responses. Section III outlines the fabrication and signal acquisition of the SnO<sub>2</sub>-ZnO sensor devices. Section IV describes the smoothing and denoising methods used. Section V provides the results of a series of systematic experiments to tune each of these signal preprocessing methods. Section VI addresses the issue of which of these preprocessing methods is most appropriate for the cleaning of MOX sensors by providing a comparison of the output signals for each of the methods using the optimal values for the tuning parameters as identified in Section V. Finally, conclusions are drawn in Section VII.

## II. BACKGROUND

While the literature on denoising and smoothing of chemical sensor signals is extensive, very little has been published specifically examining appropriate methods for denoising the gas response signals obtained from MOX sensors.

Guiñón et al. used both moving average (MA) and Savitsky Golay (SG) filters to smooth the photochemical and electrochemical reactor data [9]. They concluded that the SG filter was better than averaging because it tends to preserve data features that are usually attenuated by the MA filter and produce very little distortion in the signal. The SG filter has also been used to smooth electrocardiogram (ECG) signals and the effect of the smoothing parameters was evaluated [10]. Leo et al. [11] reported on the use of SG filters to denoise a large scale chemical sensor array prior to classifying the response signals from a variety of sensors composed of conducting polymer materials. The choice of SG filters was based on our earlier preliminary work on the use of SG filters for denoising pure SnO<sub>2</sub> and pure ZnO thin film gas sensor responses to methanol [1]. In this earlier work the use of local regression, moving average and SG filters were evaluated. Further work using these filters was reported but this time with a number of thin film SnO<sub>2</sub>-ZnO composite gas sensor devices [8]. This work resulted in the conclusion that the SG smoothing filter gave the best denoising result regardless of thin film composition, target gas concentration and device operating temperature. However, in both of these studies [1][8], the tuning parameters were not established in a thorough and systematic manner. Instead, they were chosen based on the researcher's knowledge of the data. Therefore, it is necessary to revisit this work with a view to tuning the parameters in order to obtain an optimal result.

In the past two decades much of the research in signal pre-processing of chemical sensor signals has been focused on wavelet transforms because they provide a procedure that has low memory requirements, high precision, and good reproducibility [12][13]. Wavelet based denoising was proposed by Donoho [14]. In 1997 Barclay and Bonner reported on the application of wavelet transforms to experimental spectra in the analytical chemistry domain. They compared discrete wavelet transform (DWT) with other common techniques: smoothing (SG filters) and denoising (Fourier transforms) on liquid chromatograms and electrospray mass spectra. They reported that in this context

wavelet filters are superior to the other methods evaluated. DWT has also been used as a technique for removing noise from biosensors [15]. Singh and Tiwari presented an evaluation of mother wavelets for denoising electrocardiogram (ECG) signals [16]. They reported that their wavelet denoising approach, DWT using a Daubechies mother wavelet [17] of order 8 and Donoho's hybrid SureShrink threshold selection procedure [18], effectively removed noise while retaining the necessary diagnostic information in the original ECG signal. One recent effective application of denoising based on wavelet transforms was the cleaning of GPS receiver positioning data [19]. Kim et al. used DWT with hard thresholding and a biorthogonal mother wavelet to denoise synthetically generated response signals [20]. In examining methods for smoothing MOX sensor signals Bassey, Whalley and Sallis [8], proposed that wavelets might be a suitable approach but did not investigate their usefulness. To date there has been little work that systematically compares and evaluates these methods for MOX sensor signal denoising.

As an expansion of our initial results [1][8] this paper aims to identify a general method for SnO<sub>2</sub>-ZnO composite gas sensor signal preprocessing that is applicable regardless of the sensor composition. Hence, this paper evaluates a number of potential methods for denoising SnO<sub>2</sub>-ZnO composite gas sensor devices including MA, local regression, robust local regression, SG, and wavelet transform methods. The results of extensive experiments to determine the best span sizes and degrees of polynomial for those methods is presented. Additionally, approaches to selecting the appropriate wavelet function are explored. The signal processing challenge of maintaining a balance between the measured signal variation and the disparity variation in the smoothed signals is outlined and considered within a systematic evaluation process.

## III. ACQUISITION OF THE RESPONSE SIGNALS

Five sensor devices were fabricated with different SnO<sub>2</sub>-ZnO compositions (Table I). Thin films of these composites were deposited on to a silicon wafer using a radio frequency sputtering process (similar to the reported for BaTiO<sub>3</sub>-CuO mixed oxide sensors [21]) for thirty minutes on a silicon/silicon dioxide substrate [22].

In initial experiments, each of these sensor devices was exposed to 150 parts per million of methanol vapor at 150, 250 and 350 degrees Celsius, respectively. A constant voltage of 5 volts was applied to the sensing elements while recording the sensor response to the target gas as a function of time of exposure to target gas.

TABLE I. MOLAR FRACTION COMPOSITIONS OF THE MOX SENSORS.

	Thin film composition (mole percentage)				
SnO <sub>2</sub>	100	75	50	25	0
ZnO	0	25	50	75	100
Sensor	S	S <sub>3</sub> Z <sub>1</sub>	SZ	S <sub>1</sub> Z <sub>3</sub>	Z

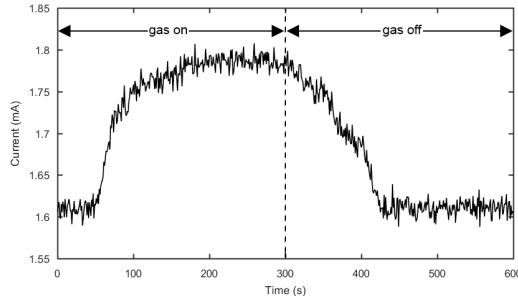
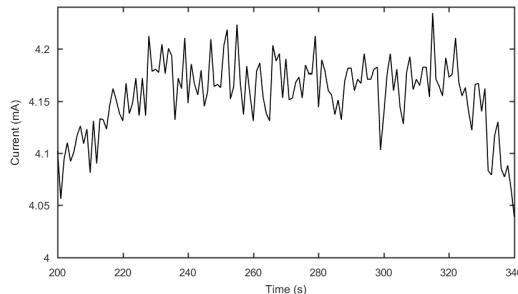


Figure 1. A typical gas sensor signal.

Figure 2. A subregion of the  $S_1Z_3$  signal illustrating typical perturbations.

Typically for calibration of MOX sensors the response is characterized using a calibration curve of the signal response (current or resistance) [23]. An unprocessed digital response from the S device, as current in milliamperes, is depicted in Fig. 1. The response data was acquired with a sampling rate of one sample per second for ten minutes. Data acquisition commenced when the target gas reached the required flow rate (the rate needed to provide the required concentration of target gas) and the gas flow was turned off after five minutes. The analog signal acquired was converted to a digital signal using a 14 bit analog to digital converter (ADC).

In initial experiments, it was found that at 150 degrees Celsius the gas response was less sensitive and that the optimal temperature of those tested for operation of these sensors was 250 degrees Celsius. For this reason the experiments for signal cleaning (denoising/smoothing) reported here use the raw signal responses obtained from the gas sensing experiments conducted at an operating temperature of 250 degrees Celsius.

Fig. 2 shows the signal noise characteristics of the  $S_3Z_1$  MOX sensor. Apart from the individual signal profile of each device, the signal noise characteristics did not exhibit any significant variation between devices. Therefore, this paper will focus on the signal processing aspects and optimization of the filter parameters.

#### IV. METHODS

The following methods, (A) polynomial curve fitting, (B) MA smoothing algorithm (C) local regression smoothing, (D) SG smoothing algorithm, and (E) wavelet denoising, were applied to the sensor response data obtained from the five MOX gas sensor devices.

##### A. Polynomial curve fitting

Arguably the simplest approach to removing noise and extracting characteristics from the raw sensor signal is to model or approximate the sensor response curve using a polynomial function. The task of selecting an appropriate degree of the polynomial is straight forward and is the only tuning required.

##### B. Moving average smoothing

One of the simplest digital filters is the MA filter. It is able to reduce random noise, through smoothing the signal, while retaining sharp step responses making it a suitable type of filter for time domain encoded signals [9]. A MA filter that is equivalent to low pass filtering was used to smooth data by replacing each data point with the average of the neighboring data points within a specified span of data points as described by the difference equation (1) where  $y_s(i)$  is the smoothed value for the  $i^{\text{th}}$  data point,  $N$  is the number of neighboring data points on either side of  $y_s(i)$ , and  $2N+1$  is the span.

$$y_s(i) = \frac{1}{2N+1} (y(i+N) + y(i+N-1) + \dots + y(i-N)) \quad (1)$$

##### C. Locally weighted regression

Locally weighted scatterplot smoothing (loess and lowess) are two non-parametric regression methods that combine multiple regression models in a k-nearest-neighbor-based meta-model [24]. For lowess and loess the smoothed values are determined by considering neighboring data points within a span. The process is weighted using a regression weight function that is defined for all the data points contained within the specified span. The span, which specifies the neighborhood as a fraction of the total number of data points, is often referred to as the smoothing parameter or bandwidth. This is the main parameter for these methods and controls the smoothness of the estimated signal in each local surrounds. Lowess and loess are differentiated by the model used in the regression: lowess uses a linear polynomial, while loess uses a quadratic polynomial.

With MA the smoothing parameter defines the span of the moving window. However, for the local regression methods the span size is given in terms of the percentage of data points in the span.

The *robust* local regression methods (rlowess and rloess) differ from lowess and loess in that a lower weight is assigned to outliers in the regression, and a zero weighting is given to data outside six mean absolute deviations. This robust approach typically gives results that are more resistant to outliers.

Experiments using loess, lowess, rloess and rlowess with span sizes of 1, 5, 8, 10, 15, and 20% of the data points were conducted in order to tune each of these methods.

##### D. Savitsky Golay smoothing

The SG smoothing algorithm is one of many other types of digital smoothing polynomials [25] and has arguably

become “an almost universal method to improve the signal-to-noise ratio of any kind of signal” [26]. The SG method [27] is a generalization of the moving average filter and is considered to be both relatively simple and have a low computational cost. It uses polynomial coefficients to determine the best least-squares fit to the points in the span. The procedure consists of replacing the central point  $p$  of a frame  $(2p+1)$  with the value obtained from the polynomial fit. The frame is moved one data point at a time, until the entire signal is scanned, creating a new smoothed value for each data point. The smoothed signal  $g(t)$  is calculated by convolving the signal  $f(t)$  with a smoothing (or convolution) function  $h(t)$  [13] for all observed data points  $p$  where  $f(m)$  is the curve function at point  $m$  and  $h(m-t) \neq 0$  (2). The convolution function  $h(t)$  is defined for each combination of degree of the polynomial and frame size.

$$g(t) = f(t) \times h(t) = \frac{\sum f(m)h(m-t)}{\sum h(m)} \quad (2)$$

In SG smoothing each data point  $f_i$  is replaced with a linear combination of  $g_i$  (3) and a number of nearby neighbors  $n$  where  $nL$  is the number of neighboring points prior to the data point  $i$ ,  $nR$  is the number of neighbors after data point  $i$ , and the coefficients  $c_n$  are the weights of the linear combination [28].

$$g_i = \sum_{n=-nL}^{nR} c_n f_{i+n} \quad (3)$$

The moving frame average (4) is computed as the average of the data points from  $f_i - nL$  to  $f_i + nR$  for some fixed  $nL = nR = M$  and the weights  $c_n = 1 / (nL + nR + 1)$  [29]:

$$g_i = \sum_{n=-M}^M \frac{f_{i+n}}{2M+1} \quad (4)$$

The weights  $c_n$  are chosen in such a way that the smoothed data point  $g_i$  is the value of a polynomial fitted by least-squares to all  $(nL + nR + 1)$  points in the moving window. That is, for the group of  $2M + 1$  data centered at  $n = 0$  the coefficient of the polynomial is obtained by (5) [30].

$$c_n = p(n) = \sum_{k=0}^N a_k n^k \quad (5)$$

This minimizes the mean-squared approximation error (6) for the group of input samples centered on  $n = 0$ .

$$\epsilon_N = \sum_{n=-M}^M (p(n) - x[n])^2 = \sum_{n=-M}^M \left( \sum_{k=0}^N a_k n^k - x[n] \right)^2 \quad (6)$$

Therefore,  $g_i$  the smoothed data [29] is given by (7).

$$g_i = \frac{\sum_{n=-nL}^{nR} c_n f_{i+n}}{\sum_{n=-nL}^{nR} c_n} \quad (7)$$

For the SG smoothing algorithm there are two tuning parameters: the frame size  $F = (nL + nR + 1)$  and the polynomial order  $k$ . The polynomial order  $k$  must be less than the frame size  $F$ , which must be odd. If  $k = F - 1$  then the designed filter produces no smoothing. Frame sizes of 5, 25, 55, 75, and 95 data points with polynomials of order 3, 6, and 9 were evaluated in order to find the optimal tuning parameters for the MOX gas sensor response signals.

### E. Wavelet denoising

Where the previously discussed methods smooth the signal by removing high frequencies and retaining low frequencies, denoising attempts to remove whatever noise is present and retain whatever signal is present regardless of the frequency content of the signal. This is essentially denoising by shrinking (nonlinear soft thresholding) in the wavelet transform domain. Third, it consists of three steps: a linear forward wavelet transform (8), a nonlinear shrinkage denoising (9), and a linear inverse wavelet transform (10). This can be defined mathematically assuming that the observed data  $x(t)$  consists of the true signal  $s(t)$  and noise  $n(t)$  as functions in time  $t$  to be sampled [31]:

$$y = W(x) \quad (8)$$

$$z = D(y, \lambda) \quad (9)$$

$$\hat{s} = W^{-1}(z) \quad (10)$$

Where  $\hat{s}(t)$  is the signal recovered as an estimate of  $s(t)$ ,  $W(\cdot)$  and  $W^{-1}(\cdot)$  are the forward and inverse wavelet transform operators respectively, and  $D(\cdot, \lambda)$  is the denoising operator with soft threshold  $\lambda$ .

One of the main considerations in wavelet denoising involves the selection of an appropriate mother wavelet function at a suitable level  $N$  and the subsequent computation of the wavelet decomposition of the signal  $s$  down to level  $N$ . There are many different types of mother wavelets available and it is important that a suitable mother wavelet is selected. The most common selection method is to visually compare the signal with potential mother wavelets and select a mother wavelet based on the degree of visual similarity. An alternate quantitative approach is to calculate the regularity, vanishing moment and degree of shift variance [32][33]. Other quantitative approaches include Satio's use of the minimum description length (MDL) as a means of selecting the optimal wavelet, from a database of orthonormal bases, for noise suppression [34]. MDL is based on an assumption that the best model is one that provides the shortest description of both the data and the model itself. Another method is to use the maximum cross correlation coefficient as a selection criterion [16][35]. To date there is no accepted standard or

generalized method for selecting the mother wavelet function [36]. In the experiments conducted here the mother wavelet was selected using the maximum cross correlation coefficient method. This approach was used after an initial selection of potential mother wavelets by visual inspection in order to ensure that the mother wavelet selected was appropriate.

The next step is to threshold, for each level from  $l$  to  $N$ , the detail coefficients. Therefore, the next important consideration is the choice of threshold selection rule [37]. A choice between hard and soft thresholding must also be made. Hard thresholding is the simpler method and results in the sharp signal features being restored but smooth regions within the signal are not always as smooth as desired. On the other hand, soft thresholding can result in over smoothing of sharp transitions but the smooth regions of the signal are restored well. It has been reported that soft thresholding tends to give better denoising results [38] for audio files. Because audio files appear to often have similar noise perturbations to those observed for the MOX sensor data it is reasonable to extrapolate that a soft thresholding approach will prove more appropriate for the preprocessing of MOX sensor gas response signals. Moreover, because we are interested in preserving the overall signal profile and in smoothing the signal more than denoising the signal a soft thresholding chooser seems to be the best option. In order to ensure that the correct thresholding chooser method was selected four commonly used choosers are evaluated:

- universal threshold selection method [14]
- minimax threshold [39]
- Stein's unbiased risk estimator (SURE) [40]
- an heuristic variant of Stein's Unbiased Risk and fixed form thresholding (heurSURE) [41]

## V. PARAMETER TUNING RESULTS

This section firstly presents the results for the tuning of the parameters for the smoothing methods and the selection of mother wavelet for wavelet denoising. All the experiments were conducted using MATLAB. All the raw data were in quantized form. The raw data or signals and denoised or smoothed signals each contained 600 data points. The best or optimal signal smoothing method was considered to be the one that best preserves the height, width, amplitude, and overall profile and data features of the signal while also reducing noise in the signal. The process for determination of "best fit" used was a visual examination. Given the data point distribution generated, this method was regarded as both adequate and appropriate. In order to assist in the determination of "best fit" the curves produced were also plotted against the 95% confidence intervals (CIs). CIs are useful in determining the precision of the predicted model and help give an idea of how useful the model is for a particular region of the data.

For the non-parametric methods, MA and the four local regression techniques, it is not possible to directly calculate CIs because the smoothed curve (model) is not based on a specific mathematical model or distribution [42]. Calculating CIs for the nonparametric methods can in principle be

achieved by viewing each fitted value as a predictor value from a regression equation and then calculating the pointwise confidence limits for each of the predicted values [43]. To plot the CIs all adjacent upper and lower confidence limits are connected with line segments in order to produce the final confidence band. It should be noted that although pointwise confidence limits do not strictly define the 'global' CIs they are known to work well, in practice, for illustrating the uncertainty in a loess curve [44].

In the following discussions we have not presented exhaustive examples of these experiments but instead have given examples to illustrate key points.

### A. Polynomial curve fitting

In order to find the best polynomial fit for the sensor response curves 3<sup>rd</sup>, 6<sup>th</sup>, and 9<sup>th</sup> degree polynomials were fitted to the response curves. The aim is to find the lowest degree polynomial that still provides a good fit to the raw signal without attenuation of the data features. The best fit for all sensor devices was that given by the 9<sup>th</sup> degree polynomial; curve fittings of less than polynomial 9 gave poor results (Fig. 4). In the case of the S sensor the fit is largely within the 95% confidence bounds for the entire profile but does not maintain the profile of the signal at the start or end of the signal (Fig. 5). The polynomial curves fit less well with the other sensor devices (e.g., Fig. 6). While the 9<sup>th</sup> degree polynomial model for the SZ sensor does not fit well in the equilibrated measurement phase (~200-300 seconds) and the initial 'gas off' period (300-400 seconds), it provides a better fit after 400 seconds, when the response returns to the base line 'off' state, than the 6<sup>th</sup> degree polynomial curve.

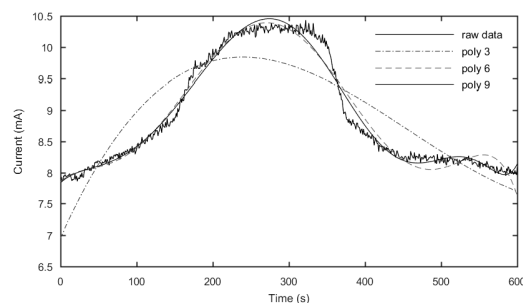


Figure 4. 3<sup>rd</sup>, 6<sup>th</sup> and 9<sup>th</sup> polynomial curve fitting for the SZ sensor response signal.

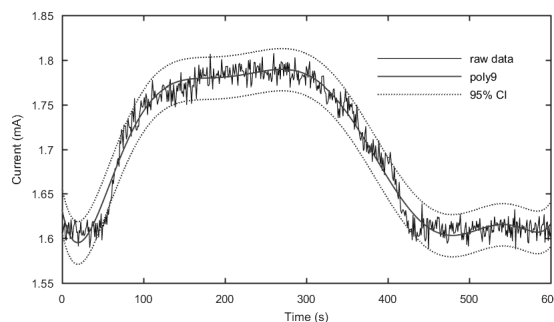


Figure 5. 9<sup>th</sup> degree fitted polynomial for the S sensor response signal.

Fig. 4 and Fig. 6 clearly illustrate that using this approach is not the best solution because it is difficult to fit the polynomial to areas of the signal that exhibit rapid change. Thus, this approach – curve fitting with simple polynomial functions – is not explored further.

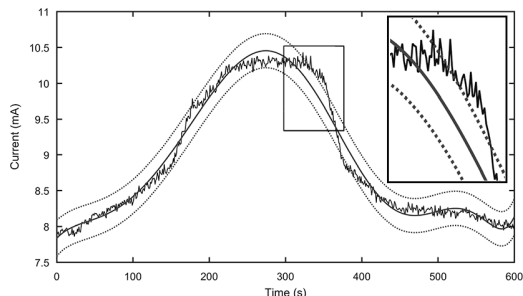


Figure 6. 9<sup>th</sup> degree fitted polynomial for the S<sub>Z</sub> sensor response signal (inset) showing data outside of the 95% CIs for the model.

### B. Moving average

To establish the optimal smoothing parameter using the MA technique span sizes of 5, 25, 55, 75, 95, and 125 data points were evaluated. Fig. 7 gives the root-mean-square error (RMSE) for each device using the MA filter with varying span sizes. As expected, as the span size increases the RMSE error increases meaning that the smoothed signal is deviating further from the profile of the original signal.

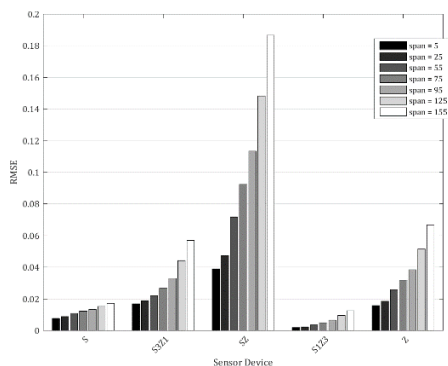


Figure 7. RMSE of the smoothed signals by device and span size.

The optimal smoothing span should therefore be the lowest possible span to ensure preservation of the profile of the raw signal and prevent loss of signal features.

MA smoothing produced the best smoothing using a span size of 25 (e.g., Fig. 8(a) and (b)). The smoothing achieved

provided an improvement on the initial reported results (see [1][8]). For all the sensors when a span size of more than 55 was used the MA filter over-smoothed the approximation and, therefore, the approximated curve did not fit as well with the raw signal and response information was lost (e.g., Fig. 8(c) and (d)).

### C. Weighted regression methods

For loess and rloess the best smoothing result was achieved with a span of 10% (Fig. 9). With a span of 1% the signal still contained perturbations that might obscure the values of the gas response features (see the  $y_{tS1_i}$  curves in Fig. 9). As the span size increases the noise in the signal becomes lower; however, using a 25% span shows that as the span size increases distortions in the signal are observed due to the smoothing filter (see the  $y_{tS25_i}$  curves in Fig. 9). Using a 20% span the resulting signal was considered to be slightly “over-smoothed”, as it did not maintain the resolution of the signal (Fig 10(c)). The other sensor devices also displayed the best loess and rloess smoothing with a 10% span (Fig. 10). This finding confirms earlier work in which a span size of 10% was suggested to be optimal for MOX sensor signal smoothing with loess and rloess filters [1][8].

The lowess filter of the S<sub>3</sub>Z<sub>1</sub>, and S and Z sensor signals exhibited the best smoothing with a 5% span. Spans of 8% and 10% gave the best smoothing for the S<sub>Z</sub> (Fig 11(a)) and S<sub>1</sub>Z<sub>3</sub> sensor signals, respectively. For rlowess the best smoothing was observed, for all the sensor devices, when a 5% span was used (e.g., the  $y_{tS5_i}$  curve in Fig. 11(b)).

Generally, above a 10% span all the local regression smoothing methods resulted in “over-smoothed” signals where noise was removed at the expense of the profile of the signal response. This results in a loss of the key diagnostic characteristics of the gas sensing signal. The results of these experiments show that different local regression smoothing methods provide optimal smoothing at different span sizes. For this reason local regression is not a viable option as a generalized method for the smoothing of MOX sensor response signals.

### D. SG smoothing

In the polynomial curve fitting experiments reported earlier in this section it was found that polynomials of less than 9 gave a poor fit for the gas response signals for all of the sensor devices. In earlier work it had been reported that SG smoothing gave the best result using a frame of size of 55 data points [1][8], with a cubic (3<sup>rd</sup> order) polynomial but neither of these parameters had been tuned to ensure that these were the optimal values. In fact, the earlier work had been restricted to frame sizes of only 5 and 55.

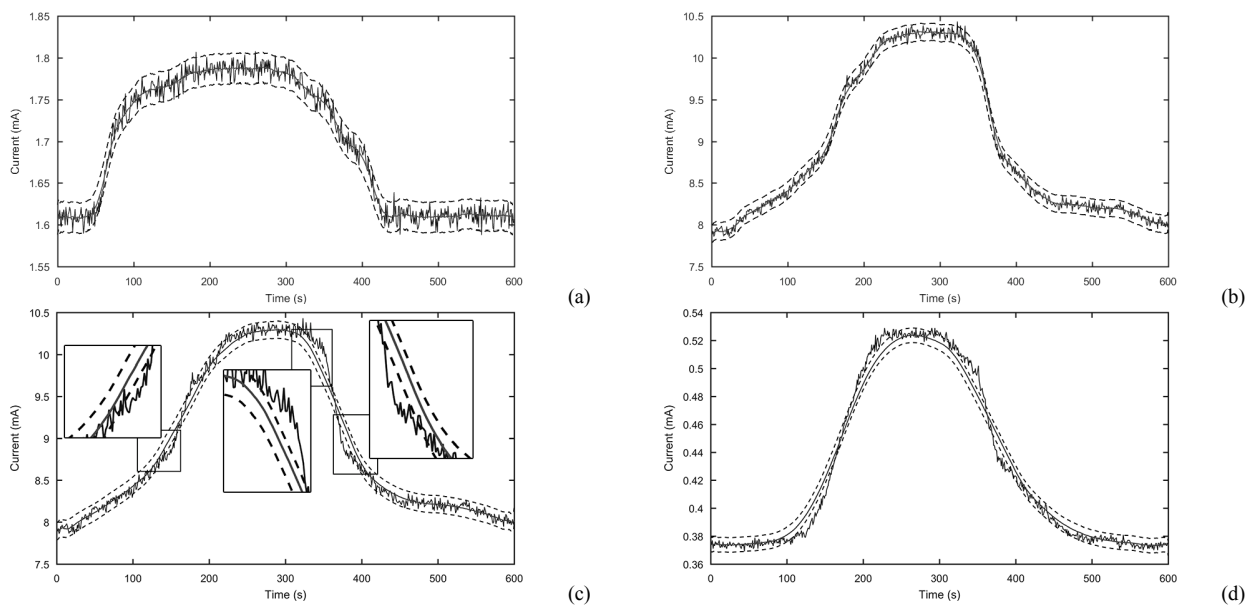


Figure 8. Raw vs smoothed signal using a MA filter: (a) S device with a span of 25, (b) SZ device with a span of 25, (c) SZ device with a span of 75 (insets) highlight some of the areas where the model is outside of the 95% confidence bands, and (d) SZZ1 device with a span of 55.

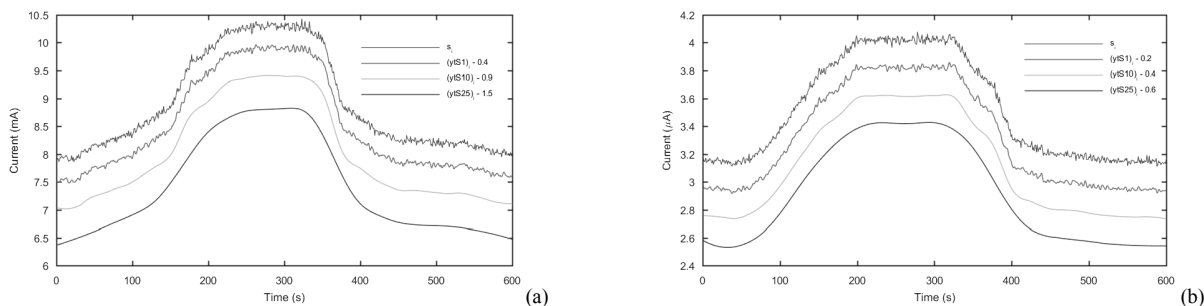


Figure 9. The same signal filtered with 1, 10 and 25% spans respectively, signals are offset for visibility: (a) noisy SZ signal vs. loess curves, (b) noisy Z signal vs. roloess curves.

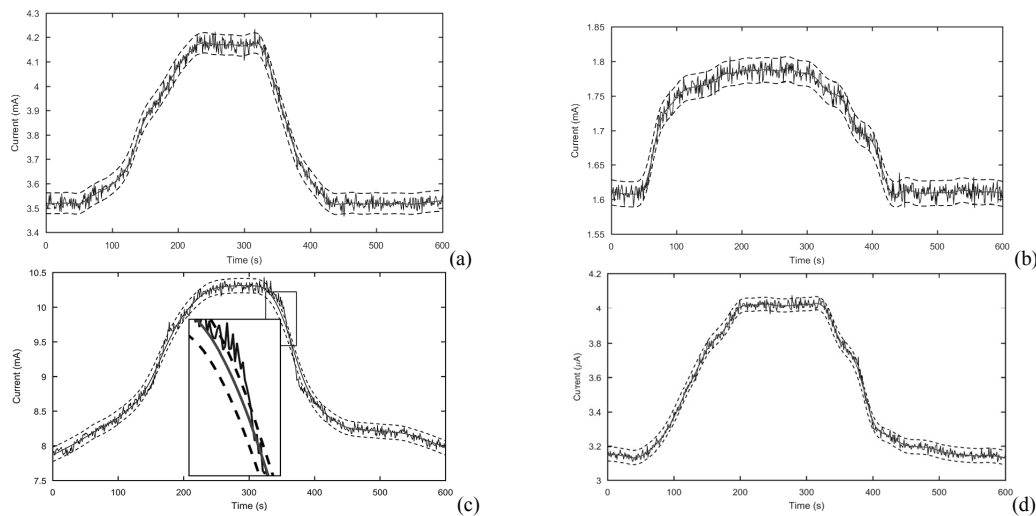


Figure 10. Smoothing with a 10% span using loess: (a) SZZ1 signal and (b) S signal and roloess curve filtering (c) SZ device signal filtering using a 20% span, (d) Z device signal filtering using a 10% span.

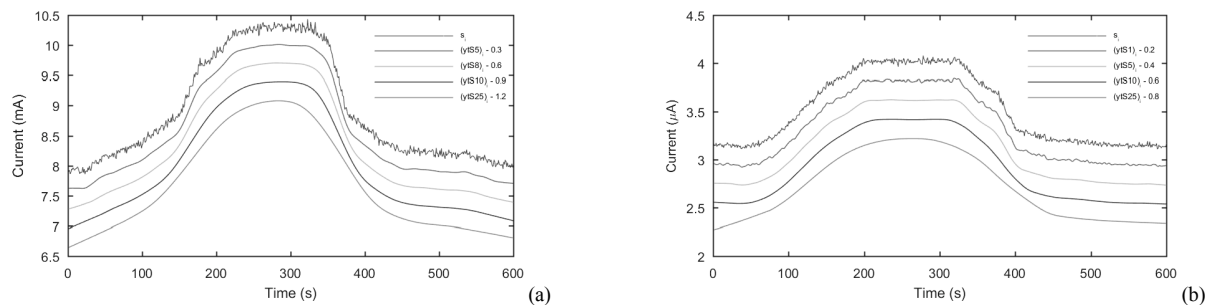


Figure 11. Raw signals vs. filtered curves, signals are offset for visibility: (a) noisy SZ signal lows filtered with 5, 8, 10 and 25% spans, (b) noisy Z signal rowless filtered with 1, 5, 10 and 25% spans.

Frame sizes  $F$  of 5, 25, 55, 75, and 95 data points with polynomials of order  $k = 3, 6,$  and  $9$  were tested in order to find the optimal tuning parameters for the SG filtering model. As a general rule of thumb it has been suggested that the best value for SG filter is the same as that for MA and that the polynomial order  $k$  should be kept as low as possible [45]. Generally, a  $k$  value should be chosen that is considerably smaller than  $F$  in order to achieve the appropriate level of smoothing and also to ensure numerical stability. Theoretically, the smaller  $k$  is in comparison to  $F$ , the greater smoothing is achieved. For our purpose, a balance needs to be made between  $k$  and  $F$  that results in a signal that preserves the raw signal's profile but also sufficiently smooths the spectra. Additionally, we require single values for  $k$  and for  $F$  that give good smoothing results across all five sensor devices.

Fig. 12 shows the influence of polynomial order  $k$  on the smoothing of the S device's gas response signal with a frame size of 25. Visual inspection shows that an order of 3, cubic, gives the best result. This confirms earlier work suggesting that optimal results are obtained with a cubic polynomial [8]. The remaining experiments therefore use a polynomial order of 3 for the SG filter. Fig. 13 shows the results of altering the frame size while keeping  $k$  constant. The smoothed signal obtained using a frame size of 25 results in a smoothed signal that still contains some perturbations, therefore, it was concluded that as reported earlier a frame size of 55 was optimal [8] as it provides a smoother signal but still maintains the profile and features of the signal.

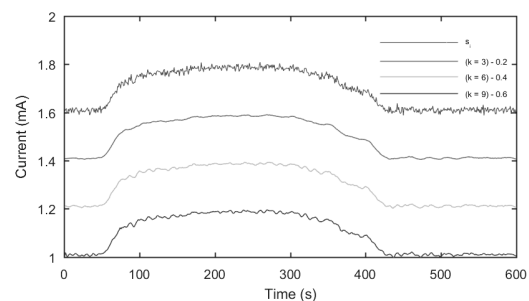


Figure 12. The effect of polynomial order on the degree of SG smoothing of the S device response signal ( $s$ ). Signals are offset for visibility.

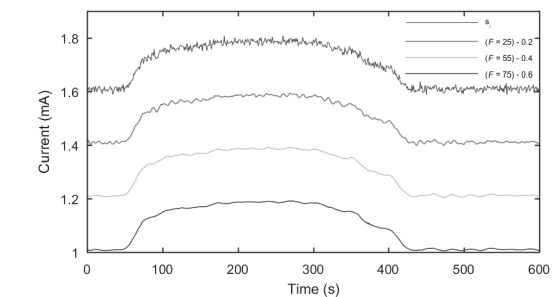


Figure 13. The effect of frame size ( $F$ ) on the level of smoothing for the S signal using a cubic polynomial. Signals are offset for visibility.

Fig. 14 depicts the SG smoothed curves for the SZ and S1Z3 devices using the optimal tuning parameter values ( $k = 3, F = 55$ ) showing that this method is suitable for all five of the MOX sensors.

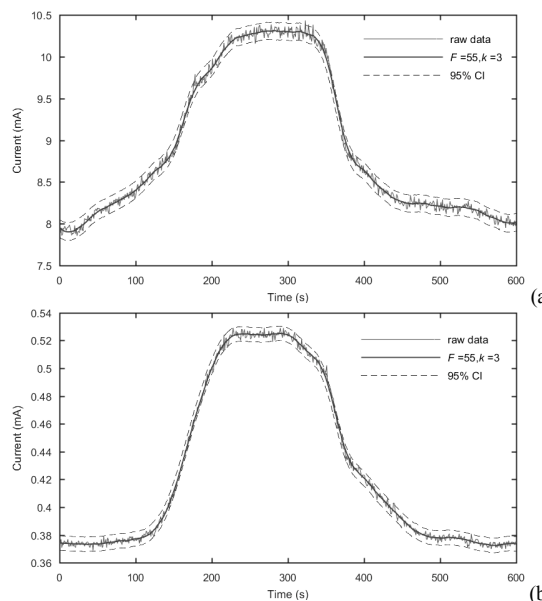


Figure 14. Plot of raw signal vs. SG smoothed signals ( $k = 3, F = 55$ ) with pointwise 95% confidence bands: (a) SZ device, (b) S1Z3 device.

E. Wavelet denoising

Visual inspection of the perturbations in the signal show that similar perturbations can be seen in the Daubechies, Symlet, and Coiflet biorthogonal families of wavelets and, therefore, they are all potential mother wavelet candidates. The cross correlation between the S gas sensor signal and the selected wavelet filter was calculated for selected wavelets from these four wavelet families (Fig. 15).

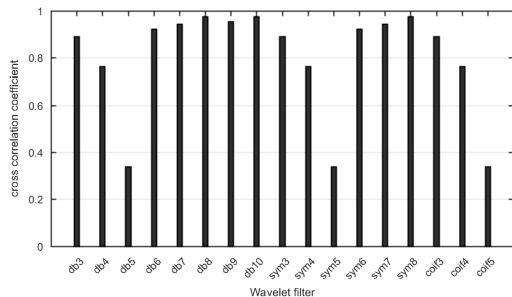


Figure 15. Comparative plot of cross correlation coefficients with selected mother wavelet filters for the S signal.

The optimum wavelet filter is one that maximizes the cross correlation coefficient [16]. Based on this cross correlation coefficient criterion, for the S gas sensor signal a Daubechies filter of order 8 (decomposition level 10) is considered to be the optimal filter. Fig. 16 is a plot of the RMSE of the denoised signals for all five devices, using a Daubechies 8 (db8) basis function with various thresholding schemes.

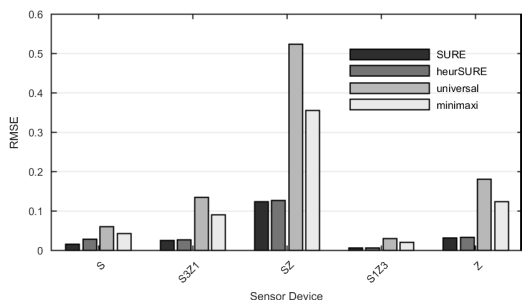


Figure 16. Comparative plot of SURE, heurSURE, universal and minimaxi thresholding schemes for all five MOX gas sensor response signals.

With the exception of the S gas sensor response signal SURE and heurSURE gave the same RMSE and performed the best as a thresholding chooser for wavelet denoising of the signals. Fig. 16 shows that for the S signal the SURE threshold chooser resulted in less difference between the denoised signal and the original signal. Therefore, the optimal wavelet denoising method for all five SnO<sub>2</sub>-ZnO composite devices sensing methanol vapor was found to be a discrete wavelet denoising approach that employed a Daubechies basis function of order 8 at a decomposition level of 10. The detail coefficients were thresholded using soft thresholding and the SURE threshold chooser with the noise scaled using a single estimation of the level of noise

based on the first-level coefficients. Fig. 17(a) and (b) compare the denoised and the original (raw) signals for the S and Z sensor devices.

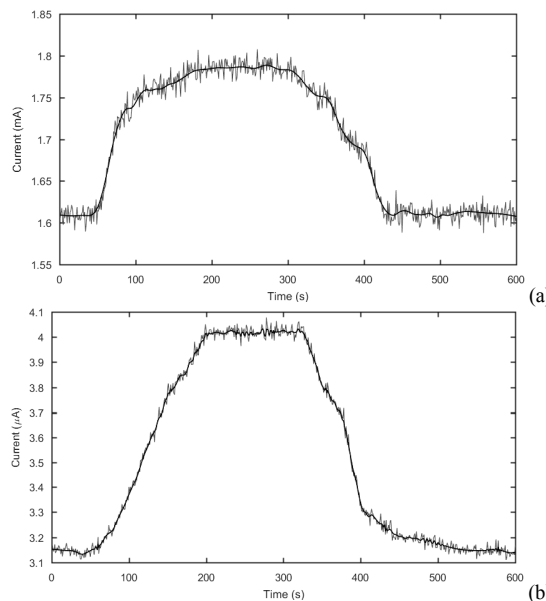


Figure 17. Plot of raw vs. wavelet denoised S (a) and Z (b) sensor signals with optimal mother wavelet (db8) and soft thresholding (with SURE).

VI. EMPIRICAL METHOD EVALUATION

In order to compare the smoothing performance of the signal pre-processing methods evaluated, the coefficient of determination ( $R^2$ ) and the RMSE were calculated for each method using the near-optimal generalized parameter values identified by this research.

$R^2$  measures the “goodness of fit” or how well the smoothed signal approximates the original signal where  $SSE$  is the sum of squared error,  $SSR$  is the sum of squared regression, and  $SST$  is the sum of squared total (11).

$$R^2 = \frac{SSR}{SST} = 1 - \frac{SSE}{SST} \tag{11}$$

The RMSE measures the differences between values estimated by the signal processing method and the values actually observed (the original signal). The RMSE represents the sample standard deviation of the differences between estimated values and the actual values (12).

$$RMSE = \sqrt{\frac{1}{n} \sum_{i=1}^n (s(n) - \hat{s}(n))^2} \tag{12}$$

For all methods and devices over 95% of the variance between the original and smoothed signals can be explained by the pre-processed model.

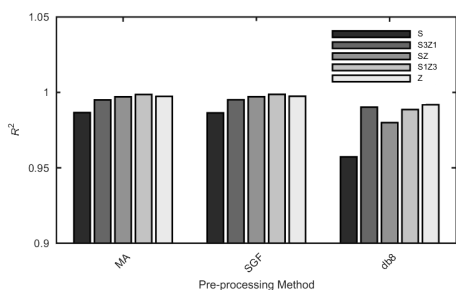


Figure 18. Coefficient of determination for the best signal pre-processing methods using the near-optimal generalized tuning parameter values.

Based on the  $R^2$  statistic the tuned MA and SG methods gave the best processed signals for all devices (Fig. 18) while the wavelet denoising approach performed slightly less well.

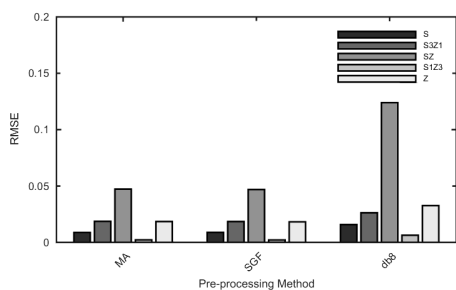


Figure 19. RMSE for the best signal pre-processing methods using the near-optimal generalized tuning parameter values.

Fig. 19 shows that for all the methods similar RMSEs were observed for each of the devices and methods with the exception of the SZ device with wavelet denoising. Denoising the SZ sensor using the db8 wavelet method resulted in the greatest difference between original and processed signal observed of all sensor/method combinations evaluated.

In determining which method holds the most promise as a generalised approach for MOX gas response signal pre-processing a balance must be found between the goodness of fit of the processed signal to the actual raw signal, the simplicity and practicality of the method, and the degree to which the method preserves the features and profile of the original signal. As discussed, the best way to determine the quality of the signal pre-processing (smoothing or denoising) is to use a visual inspection of the processed signal. If we used a purely statistical approach ( $R^2$  and RMSE) then the best approach appears to be either SG smoothing or MA. Given that a moving average approach is simpler than SG, it is tempting to assume that MA offers the most promising generalised approach. However, visual examination of the results of smoothing showed that the SG gives a better smoothing result than MA because it maintains the features and profile of the signal better when considering the consistency in the quality of the smoothing regardless of device composition (as discussed in Section V).

While wavelet denoising appears to lack sufficient consistency in results across the different sensor devices' MOX compositions, visual inspection of the denoised signals suggests that wavelet denoising is a plausible alternative to SG smoothing. It should also be noted that even though wavelet denoising of the SZ sensor has a lower  $R^2$  and a higher RMSE, the difference in fit and error between it and the other sensors is actually minimal.

Fig. 20 shows plots for the wavelet denoising of the SZ sensor signal (the worst wavelet denoising result) and the  $S_3Z_1$  sensor (the best wavelet denoising result).

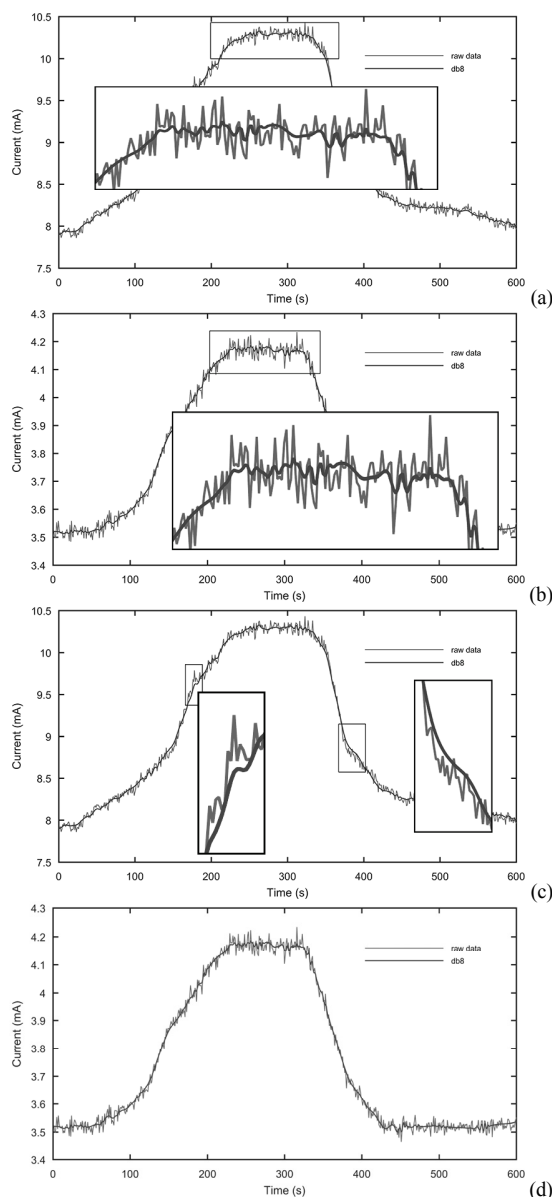


Figure 20. Plot of db8 wavelet denoised signals with original response signal for: (a) SZ sensor and (b)  $S_3Z_1$  sensor (insets show perturbations), (c) SZ sensor (insets highlight regions where the profile of the original curve is not maintained) and (d) the full  $S_3Z_1$  signal.

The insets provided in Fig. 20(a) and (b) show an enlarged view of the perturbations remaining in the denoised signals. Fig. 20(c) contains insets that highlight some of the regions in the denoised signal where it deviates from the profile of the original raw response signal. If the  $SZ$  signal is compared with the  $S_{3Z1}$  signal it can be seen that the denoised  $SZ$  signal has a poorer fit than the denoised  $S_{3Z1}$  signal. Both denoised signals appear to have a very similar degree of smoothing. Less smoothing of the signal is observed using the wavelet approach than when using a SG filter (Fig. 14) but the wavelet denoised signal preserves the features and the profile of the original signal well.

## VII. CONCLUSION AND FUTURE WORK

In this paper, an optimal wavelet basis function was applied to a set of MOX gas sensor response signals generated by exposing the sensor devices to methanol. The results revealed that a Daubechies mother wavelet of order 8 gives a reasonable compromise solution across all the sensor device compositions, suggesting that this might be a suitable method for other metal oxide sensor responses and for devices exposed to other gases as a signal pre-processing step. In order to establish whether or not such an approach is appropriate in practice further study is required to determine how generalizable the method is. Even if wavelets proved to be suitable there may still be complications in the implementation due to the need to select the order of the mother wavelet, level of decomposition of the wavelet coefficients, and thresholding method because these may differ for different MOX sensor compositions and gases.

While the wavelet denoising approach gives good results, it is a more complex process than the other more traditional moving average and regression approaches evaluated in this paper.

The alternative methods investigated do not pose the same degree of challenge in implementation and tuning that denoising using wavelets does. Among these approaches, SG smoothing looks to be the most promising as it resulted in a smoothed signal that maintained the profile of the original signal, and yielded near-optimal tuning parameter values that could be used regardless of sensor composition. SG smoothing was also found to give more consistent results than the wavelet approach, resulting in the removal of more of the perturbations in the signal. These perturbations have the potential to make subsequent feature extraction and pattern recognition difficult. Moreover, because SG is a much simpler approach and the tuning of the parameters is relatively straightforward it should be possible to automate the tuning process. Some work has already been reported in the literature towards automating tuning of the smoothing parameters [26]. This makes the SG smoothing approach (using a frame size of 55 data points/9% of the signal and a polynomial of 3) a more pragmatic solution to the pre-processing of MOX gas sensor response signals than wavelet denoising.

In order to substantiate further the usefulness of the SG approach the methods future work should include an evaluation of the method using signals produced by MOX

sensors of different compositions and various gases (e.g., ethanol vapor). Finally, the Daubechies wavelet approach is also worth investigating further in order to see if an automated approach to selecting the mother wavelet and tuning of parameters is possible to simplify the practical application of the method.

## ACKNOWLEDGMENT

We thank the School of Computer and Mathematical Sciences for the postgraduate summer internship funding that, in part, supported this research.

## REFERENCES

- [1] E. Bassey, J. Whalley, and P. Sallis, "An Evaluation of Smoothing Filters for Gas Sensor Signal Cleaning," The Fourth Int. Conf. Adv. Commun. Comput. (INFOCOMP 2014) IARIA, pp. 19–23, 2014.
- [2] C. Wang, L. Yin, L. Zhang, D. Xiang, and R. Gao, "Metal Oxide Gas Sensors: Sensitivity and Influencing Factors," *Sensors*, vol. 10, no. 3, pp. 2088–2106, 2010.
- [3] S. Sharma and M. Madou, "A new approach to gas sensing with nanotechnology," *Philos. Trans. A. Math. Phys. Eng. Sci.*, vol. 370, no. 1967, pp. 2448–73, 2012.
- [4] A. Gutierrez Galvez, "Coding and learning of chemosensor array patterns in a neurodynamic model of the olfactory system," Texas A&M University, Texas, United States, 2006.
- [5] R. Gutierrez-Osuna, "Pattern analysis for machine olfaction: A review," *IEEE Sens. J.*, vol. 2, no. 3, pp. 189–202, 2002.
- [6] V. J. Barclay, R. F. Bonner, and I. P. Hamilton, "Application of Wavelet Transforms to Experimental Spectra: Smoothing, Denoising, and Data Set Compression," *Anal. Chem.*, vol. 69, no. 1, pp. 78–90, Jan. 1997.
- [7] I. Garcia-Perez, M. Vallejo, A. Garcia, C. Legido-Quigley, and C. Barbas, "Metabolic fingerprinting with capillary electrophoresis," *J. Chromatogr. A*, vol. 1204, no. 2, pp. 130–139, Sep. 2008.
- [8] E. Bassey, J. Whalley, P. Sallis, and K. Prasad, "Wavelet Transform Smoothing Filters for Metal Oxide Gas Sensor Signal Cleaning," The 8th Int. Conf. Sens. Technol., pp. 2–4, 2014.
- [9] J. L. Guiñón, E. Ortega, J. García-Antón, and V. Pérez-herranz, "Moving Average and Savitzki-Golay Smoothing Filters Using Mathcad," *The Int. Conf. Eng. Educ.*, no. 1, pp. 1–4, 2007.
- [10] M. Awal, S. Mostafa, and M. Ahmad, "Performance Analysis of Savitzky-Golay Smoothing Filter Using ECG Signal," *Int. J. Comput. Inf. Technol.*, vol. 01, no. 02, pp. 90–95, 2011.
- [11] M. Leo, C. Distanto, M. Bernabei, and K. Persaud, "An efficient approach for preprocessing data from a large-scale chemical sensor array," *Sensors (Basel)*, vol. 14, no. 9, pp. 17786–806, 2014.
- [12] L. Bao, J. Mo, and Z. Tang, "The Application in Processing Analytical Chemistry Signals of a Cardinal Spline Approach to Wavelets," *Anal. Chem.*, vol. 69, no. 15, pp. 3053–3057, Aug. 1997.
- [13] C. Perrin, B. Walczak, and D. L. Massart, "The Use of Wavelets for Signal Denoising in Capillary Electrophoresis," *Anal. Chem.*, vol. 73, no. 20, pp. 4903–4917, Oct. 2001.
- [14] D. L. Donoho, "De-noising by Soft-thresholding," *IEEE Trans. Inf. Theor.*, vol. 41, no. 3, pp. 613–627, May 1995.
- [15] A. V Jagtiani, R. Sawant, J. Carletta, and J. Zhe, "Wavelet transform-based methods for denoising of Coulter counter signals," *Meas. Sci. Technol.*, vol. 19, no. 6, p. 65102, 2008.

- [16] B. N. Singh and A. K. Tiwari, "Optimal selection of wavelet basis function applied to ECG signal denoising," *Digit. Signal Process. A Rev. J.*, vol. 16, no. 3, pp. 275–287, 2006.
- [17] I. Daubechies, *Ten Lectures on Wavelets*. Philadelphia, PA, USA, PA, USA: Society for Industrial and Applied Mathematics, 1992, doi: 10.1137/1.9781611970104.
- [18] D. Donoho and I. Johnstone, "Adapting to Unknown Smoothness via Wavelet Shrinkage," *J. Am. Stat. Assoc.*, vol. 90, no. 432, pp. 1200–1224, 1995.
- [19] M. R. Mosavi and I. Emamgholipour, "De-noising of GPS Receivers Positioning Data Using Wavelet Transform and Bilateral Filtering," *Wirel. Pers. Commun.*, vol. 71, no. 3, pp. 2295–2312, Aug. 2013.
- [20] H. Kim, B. Konnanath, P. Sattigeri, J. Wang, A. Mulchandani, N. Myung, M. a. Deshusses, A. Spanias, and B. Bakkaloglu, "Electronic-nose for detecting environmental pollutants: Signal processing and analog front-end design," *Analog Integr. Circuits Signal Process.*, vol. 70, no. 1, pp. 15–32, 2012.
- [21] S. B. Rudraswamy, P. K. Basu, and N. Bhat, "Sensitivity characteristics of Ag doped BaTiO<sub>3</sub>-CuO mixed oxide as carbon-dioxide sensor," *Electronics, Computing and Communication Technologies (IEEE CONECCT)*, 2014 IEEE International Conference on. pp. 1–4, 2014.
- [22] E. Basse, P. Sallis, and K. Prasad, "Analysis of Methanol Sensitivity on SnO<sub>2</sub>-ZnO Nanocomposite," in *Characterization of Minerals, Metals, and Materials*, Hoboken, NJ, USA: John Wiley & Sons, Inc., 2016, doi: 10.1002/9781119263722.ch35
- [23] G. Neri, A. Bonavita, G. Micali, G. Rizzo, E. Callone, and G. Carturan, "Resistive CO gas sensors based on In<sub>2</sub>O<sub>3</sub> and InSnOx nanopowders synthesized via starch-aided sol-gel process for automotive applications," *Sensors Actuators B Chem.*, vol. 132, no. 1, pp. 224–233, May 2008.
- [24] W. S. Cleveland, "Robust Locally Weighted Regression and Smoothing Scatterplots," *J. Am. Stat. Assoc.*, vol. 74, no. 368, pp. 829–836, 1979.
- [25] H. Ziegler, "Properties of Digital Smoothing Polynomial (DISPO) Filters," *Appl. Spectrosc.*, vol. 35, no. 1, pp. 88–92, 1981.
- [26] G. Vivó-Truyols and P. J. Schoenmakers, "Automatic Selection of Optimal Savitzky-Golay Smoothing," *Anal. Chem.*, vol. 78, no. 13, pp. 4598–4608, Jul. 2006.
- [27] A. Savitzky and M. J. E. Golay, "Smoothing and Differentiation of Data by Simplified Least Squares Procedures," *Anal. Chem.*, vol. 36, no. 8, pp. 1627–1639, Jul. 1964.
- [28] W. H. Press, S. A. Teukolsky, W. T. Vetterling, and B. P. Flannery, *Numerical Recipes 3rd Edition: The Art of Scientific Computing*, New York, NY, USA: Cambridge University Press, 2007.
- [29] M. Zuppa, "Drift counteraction with multiple self-organising maps for an electronic nose," *Sensors Actuators B Chem.*, vol. 98, no. 2–3, pp. 305–317, Mar. 2004.
- [30] R. W. Schafer, "What is a savitzky-golay filter?," *IEEE Signal Process. Mag.*, vol. 28, no. 4, pp. 111–117, 2011.
- [31] C. Taswell, "The what, how, and why of wavelet shrinkage denoising," *Comput. Sci. Eng.*, vol. 2, no. 3, pp. 1–11, 2000.
- [32] S. Fu, B. Muralikrishnan, and J. Raja, "Engineering Surface Analysis With Different Wavelet Bases," *J. Manuf. Sci. Eng.*, vol. 125, no. 4, pp. 844–852, Nov. 2003.
- [33] S.-Y. Wang, X. Liu, J. Yianni, T. Z. Aziz, and J. F. Stein, "Extracting burst and tonic components from surface electromyograms in dystonia using adaptive wavelet shrinkage," *J. Neurosci. Methods*, vol. 139, no. 2, pp. 177–184, Oct. 2004.
- [34] N. Saito, "Simultaneous noise suppression and signal compression using a library of orthonormal bases and the minimum description length criterion," *Wavelets Geophys.*, vol. 4, pp. 299–324, 1994.
- [35] W. Li, "Research on Extraction of Partial Discharge Signals Based on Wavelet Analysis," *Electronic Computer Technology*, 2009 International Conference on. pp. 545–548, 2009.
- [36] W. K. Ngui, M. S. Leong, L. M. Hee, and A. M. Abdelrhman, "Wavelet Analysis: Mother Wavelet Selection Methods," *Appl. Mech. Mater.*, vol. 393, pp. 953–958, 2013.
- [37] G. Nason, "Choice of the Threshold Parameter in Wavelet Function Estimation," *Wavelets Stat. Lect. Notes*, vol. 103, pp. 261–280, 1995.
- [38] R. Aggarwal and S. Rathore, "Noise Reduction of Speech Signal using Wavelet Transform with Modified Universal Threshold," *Int. J. Comp. App.*, vol. 20, no. 5, pp. 14–19, 2011.
- [39] D. L. Donoho and I. M. Johnstone, "Minimax estimation via wavelet shrinkage," *Ann. Stat.*, vol. 26, no. 3, pp. 879–921, 1998.
- [40] C. Stein, "Estimation of the Mean of a Multivariate Normal Distribution," *Ann. Stat.*, vol. 9, no. 6, pp. 1135–1151, 1981.
- [41] S. G. Chang, B. Yu, and M. Vetterli, "Adaptive wavelet thresholding for image denoising and compression," *IEEE Trans. Image Process.*, vol. 9, no. 9, pp. 1532–1546, 2000.
- [42] M. Nicolich and G. Jorgensen, "Graphical Presentation of a Nonparametric Regression with Bootstrapped Confidence Intervals," 23<sup>rd</sup> Annual SAS Users Group International, Statistics, Data Analysis, and Modeling, no. 1979, pp. 1–5, 1989.
- [43] W. G. Jacoby, "Loess: A nonparametric, graphical tool for depicting relationships between variables," *Elect. Stud.*, vol. 19, no. 4, pp. 577–613, 2000.
- [44] N. Beck and S. Jackman, "Getting the mean right is a good thing: generalized additive models," *Soc. Polit. Methodol.* [Online]. Available from: <http://polmeth.wustl.edu/files/polmeth/beck97.pdf> 2016.05.26
- [45] D. Wilson, "The black art of smoothing," *Electr. Autom. Technol.*, June/July Issue, pp. 35–36, 2006.